

Implication of the Central Nucleus of the Amygdala in Cardiovascular Regulation and Limiting Maximum Exercise Performance During High-intensity Exercise in Rats

Kei Tsukioka,^{a,b} Ko Yamana^a and Hidefumi Waki^{a,c,*}

^a Department of Physiology, Graduate School of Health and Sports Science, Juntendo University, Chiba 270-1695, Japan

^b Research Fellow of Japan Society for the Promotion of Science, Tokyo 102-0083, Japan

^c Institute of Health and Sports Science & Medicine, Juntendo University, Chiba 270-1695, Japan

Abstract—To date, the mechanism of central fatigue during high-intensity exercise has remained unclear. Here we elucidate the central mechanisms of cardiovascular regulation during high-intensity exercise with a focus on the hypothesis that amygdala activation acts to limit maximum exercise performance. In the first of three experiments, we probed the involvement of the central nucleus of the amygdala (CeA) in such regulation. Wistar rats were subjected to a maximum exercise test and their total running time and cardiovascular responses were compared before and after bilateral CeA lesions. Next, probing the role of central pathways, we tested whether high-intensity exercise activated neurons in CeA and/or the hypothalamic paraventricular nucleus (PVN) that project to the nucleus tractus solitarius (NTS). Finally, to understand the potential autonomic mechanisms affecting maximum exercise performance, we measured the cardiovascular responses in anesthetized rats to electrical microstimulation of the CeA, PVN, or both. We have found that (1) CeA lesions resulted in an increase in the total exercise time and the time at which an abrupt increase in arterial pressure appeared, indicating an apparent suppression of fatigue. (2) We confirmed that high-intensity exercise activated both the PVN-NTS and CeA-NTS pathways. Moreover, we discovered that (3) while stimulation of the CeA or PVN alone both induced pressor responses, their simultaneous stimulation also increased muscle vascular resistance. These results are evidence that cardiovascular responses during high-intensity exercise are affected by CeA activation, which acts to limit maximum exercise performance, and may implicate autonomic control modulating the PVN-NTS pathway via the CeA. © 2022 IBRO. Published by Elsevier Ltd. All rights reserved.

Key words: cardiovascular regulation, central nucleus of amygdala, high-intensity exercise, hypothalamic paraventricular nucleus, nucleus tractus solitarius.

INTRODUCTION

Prolonged or high-intensity exercise induces extreme fatigue. Fatigue is generally understood to be of two types, one that originates peripherally, the other, centrally. Peripheral fatigue manifests in decreased exertion of muscle strength caused by peripheral factors, including locally produced metabolites, and the

underlying mechanisms have been previously investigated (Westerblad et al., 1991; Fitts, 1994; Allen et al., 2008). Not much is known regarding central fatigue. It is considered that the negative emotions that arise during such hard exercise directly influence motivation for continuing exercise. However, it should be noted that mental events are strongly associated with autonomic cardiovascular responses; therefore, emotion-related autonomic changes may interrupt the ideal hemodynamic homeostasis in the active skeletal muscle, contributing to and facilitating muscle fatigue.

The central nucleus of the amygdala (CeA) in the limbic system is known to play a role in emotional control (Baxter and Murray, 2002; LeDoux, 2007; DiFeliceantonio and Berridge, 2012; Mahler and Berridge, 2012; Fadok et al., 2018) in general and is associated with negative emotions (Ciocchi et al., 2010; Duvarci et al., 2011; Li et al., 2013; Duvarci and Pare, 2014; Krabbe et al., 2018; Gu et al., 2020) in particular.

*Correspondence to: H. Waki, Department of Physiology, Graduate School of Health and Sports Science, Juntendo University, 1-1 Hiraka-gakuidai, Inzai, Chiba 270-1695, Japan.

E-mail addresses: k-yamana@juntendo.ac.jp (K. Yamana), hwa-ki@juntendo.ac.jp (H. Waki).

Abbreviations: AAV, adeno-associated virus; BT, body temperature; CeA, central nucleus of the amygdala; CTB, cholera toxin subunit B; CVLM, caudal ventrolateral medulla; HR, heart rate; MAP, mean arterial pressure; MBF, muscle blood flow; NTS, nucleus tractus solitarius; PBS, phosphate-buffered saline; PFA, paraformaldehyde; PVN, hypothalamic paraventricular nucleus; RVLM, rostral ventrolateral medulla; Time-BPinc, time of abrupt increase in MAP; VR, vascular resistance.

Recently, we revealed that c-Fos expression, a marker of neuronal activity, was exaggerated in the CeA in response to prolonged and high-intensity exercise but not to low-intensity exercise (Kim et al., 2020). Thus, CeA activation may be related to negative emotions during high-intensity exercise. Additionally, the CeA regulates the cardiovascular system (Saha, 2005). Specifically, the CeA innervates the nucleus tractus solitarius (NTS), which is one of the centers of cardiovascular regulation (Rogers and Fryman, 1988) and regulates autonomic nerve activity, arterial pressure, and heart rate (HR) (Waki et al., 2003). A previous study by our group revealed that electrical and chemical stimulation of the CeA increased arterial pressure and HR (Yamanaka et al., 2018).

Moreover, the hypothalamic paraventricular nucleus (PVN), which projects to the NTS, is one of the brain areas related to psychological and/or physiological stress and cardiovascular regulation (Silverman et al., 1981; Kannan and Yamashita, 1985). In addition, the PVN is known to be involved in exercise-related central command control of sympathetic nerve activity via both direct and indirect projections to sympathetic preganglionic neurons in the intermediolateral cell column (Michelini and Stern, 2009; Dampney et al., 2018). Interestingly, a previous study showed that c-Fos expression in the PVN increased in proportion to exercise intensity (Lima et al., 2019).

In this study, we hypothesized that the activation of the CeA during high-intensity exercise affects cardiovascular regulation by mediating the PVN and NTS interactions, and, as a result, affects maximum exercise performance. We conducted three experiments to test this hypothesis. First, to investigate the role of the CeA in response to high-intensity exercise, we examined exercise performance and cardiovascular responses to incremental exercise before and after bilateral CeA lesions. Second, to explore the central pathways of cardiovascular regulation during high-intensity exercise, we tested whether the NTS-projecting CeA and/or PVN neurons were activated by high-intensity exercise using immunohistochemistry. Finally, to understand the potential autonomic mechanisms of cardiovascular responses and estimate how they affect maximum exercise performance through the CeA, we measured the hemodynamic responses to electrical microstimulation of the CeA, the PVN, and both brain areas in anesthetized rats.

Our results provide early support to our central hypothesis and suggest that the CeA may partake in the autonomic control of exercise-dependent cardiovascular regulation to limit maximum exercise performance.

EXPERIMENTAL PROCEDURES

Animals

Thirty-two male Wistar rats (age 7–11 weeks; weight: 169.8 ± 5.7 g; Japan SLC, Shizuoka, Japan) were included in the study. The animals were housed in standard cages in a temperature-controlled environment (room temperature: 24 ± 1 °C; humidity: $55 \pm 5\%$)

under a fixed 12/12-hour dark/light cycle (6:00–18:00/18:00–6:00), and were provided with *ad libitum* access to food (Rodent LabDiet EQ, 5L37, PMI Nutrition International, MO, USA) and water, except when on a treadmill and for 90 min after exercise. The study was conducted in accordance with the guidelines of the Japan Physiological Society with the approval of the Animal Experiment Ethics Committee of Juntendo University (approval ID: H29-02, H30-05). Animal suffering and the number of animals needed to obtain reliable results were kept at a minimum.

Protocols

The overall protocol to investigate the effect of bilateral CeA lesions on the total treadmill running time and cardiovascular responses during exercise was as follows. First, a radio transmitter was implanted in the rats at 7–8 weeks of age. Five to seven days later, the first treadmill exercise was performed. Subsequently, bilateral CeA lesions were made electrically. Finally, the rats performed the treadmill exercise the second time at 11 weeks of age.

Grouping for the treadmill exercise test

Bilateral CeA lesion and sham operation groups were used in this study. The grouping was adjusted to ensure that the exercise time during the pretest was the same in both the groups. Additionally, the mean arterial pressure (MAP) and HR resting levels before the exercise test were similar between the two groups.

Incremental exercise test

First, the rats were familiarized with the treadmill (55 cm W × 10 cm D, width measured from the shock grid; model MK-680; Muromachi Kikai, Tokyo, Japan) using a habituation protocol lasting 60 min per day for 3 days. Rats were made to start running at an initial speed of 10 m/min, and the speed was increased every 10 min by 2 m/min increments up to a ceiling of 20 m/min.

After habituation, an incremental exercise test was conducted. Following an initial 60 min rest time, the exercise intensity was started at 10 m/min, and the speed was increased by 2 m/min steps every 3 min. The animal's running position on the treadmill was determined by movie analysis using DeepLabCut (Mathis et al., 2018). The exercise test terminated when the rats either received electric shocks from the grid at the back of the treadmill for 10 s or could not keep pace with the belt.

The above habituation-exercise protocol was repeated a second time five or more days after the CeA lesion surgery.

Surgical anesthesia

Anesthesia was induced with pentobarbital sodium (60 mg/kg intraperitoneal [IP] injection) and maintained with isoflurane (1.0–3.0%, Pfizer, NY, USA) using an inhalation anesthesia apparatus (Univentor 400 isoflurane anesthesia unit; Univentor, Zejtun, Malta).

The level of anesthesia was checked frequently by assessing limb withdrawal reflexes to noxious pinching.

Surgical implantation of radio transmitter

To monitor cardiovascular parameters, including HR, from continuously measured arterial pressure, the rats were catheterized in the abdominal aorta and implanted with a radio transmitter (HD-S10; Data Sciences International, St. Paul, MN, USA) under anesthesia, as described previously (Waki et al., 2003; Yamanaka et al., 2018; Tsukioka et al., 2019; Kim et al., 2020). The catheter was secured in the aorta with tissue adhesive Vetbond (3M, MN, USA) and a cellulose patch. After surgery, antibiotics (1000-U benzylpenicillin, intramuscular injection; Meiji Seika Pharma, Japan) and analgesics (1 mg/kg meloxicam, subcutaneous injection; Boehringer Ingelheim, Germany) were administered and the rats were returned to their cages for recovery for 5–7 days.

CeA lesions

Animals were placed under anesthesia (as described above) in a stereotaxic head holder (SR6R-HT; Narishige Scientific Instrument Lab, Tokyo, Japan), and a concentric microelectrode (OA212-053a; Unique Medical, Tokyo, Japan) was inserted into the CeA (1.8 mm caudal, 3.0 mm lateral to the bregma, and 7.0 mm ventral to the dura) on both hemispheres. We used this coordinate because this area of the CeA has been previously shown to affect blood pressure and HR (Yamanaka et al., 2018). Furthermore, it has been reported that the region connected to the NTS, which is a circulatory control center, is the inner region of the CeA (Gasparini et al., 2020). In the CeA lesion group ($n = 8$), electrolytic currents were passed (1 mA of DC current for 5 s). In the sham group ($n = 7$), the tip of the electrode was inserted into the CeA, and immediately removed without electrical microstimulation.

Postmortem histological localization of the CeA lesions sites

After completing the experimental protocol, rats were euthanized (transcardially perfused with phosphate-buffered saline (PBS, 50 ml) followed by 4% paraformaldehyde (PFA, 50 ml) under deep isoflurane anesthesia). The brains were removed and sliced into 50 μm serial sections using a microtome (REM-710; Yamato Kohki Industrial, Saitama, Japan). Sections were mounted on slides and imaged using a fluorescence microscope (EVOS FL Auto 2 Cell Imaging System, Thermo Fisher Scientific, MA, USA). Lesion marks were detected and their anatomical loci in the CeA were identified visually.

Calculating the time of an abrupt increase of mean arterial pressure (MAP)

The time of the abrupt increase in MAP was calculated by detecting the “change point” of the MAP during exercise using a MATLAB function (<https://mathworks.com/help/signal/ref/findchangepts.html>) that returns the index into

a discrete series of data points at which the local mean changes most significantly. If exercise was completed without an abrupt increase in MAP and its time was undefined, we assigned it the default value defined as equal to the total running time.

Immunohistochemistry

In this dual-label design, NTS-projecting neurons in the CeA or PVN were detected by the presence of a fluorophore-conjugated retrograde tracer stereotaxically injected in the NTS (0.5 mm rostral, 0.5 mm lateral to the area postrema, and 0.5 mm ventral to the dorsal surface of the brain stem), and their exercise-induced activity was measured by the level of c-Fos expression gauged with a fluorescent c-Fos antibody stain.

The retrograde tracer, cholera toxin subunit B (CTB) conjugated to Alexa Fluor 488 (1% weight /volume, Thermo Fisher Scientific, MA, USA) was delivered with stereotaxic injection (200 nl in each side; 24 s) into the NTS of rats ($n = 11$) under anesthesia (as described above). Four to five days after the CTB injection, rats in the exhaustion group ($n = 6$) were subjected to an incremental exercise test, and rats in the control group ($n = 5$) spent 2 h on the treadmill without running. The rats were returned to their cages and waited for 90 min (time sufficient for c-Fos expression to occur), and then euthanized (as described for lesion localization). Brains were extracted, dissected, and stored in fixative at 4 °C (first in 4% PFA, and then transferred to a 30% sucrose solution). Fixed brains were serially cut into 50 μm sections using a microtome (REM-710, Yamato Kohki Industrial, Saitama, Japan), soaked and stored in PBS at 4 °C.

Slices were washed in PBS (5 min; 3 times), placed in PBS with 10% horse or goat serum and 0.3% Triton-X for 20 min, and then incubated overnight with an immunostaining enhancer (IMMUNO SHOT Fine, IS-F-20; Cosmo Bio, Tokyo, Japan) and the primary anti-c-Fos antibody (either goat, 0.5%; sc-52-G, Santa Cruz Biotechnology Inc., CA, USA; or rabbit, 0.05%; RPCA-c-Fos, Encor Biotechnology Inc., FL, USA). After a second PBS-wash (5 min; 3 times), slices were incubated (1 h) with Immunoshot Fine and the secondary antibody (either 0.2% biotinylated horse anti-goat c-Fos IgG, BA-9500; Vector Laboratories, CA, USA; or 0.2% biotinylated goat anti-rabbit c-Fos IgG, BA-1000; Vector Laboratories, CA, USA). Following another round of PBS-wash (5 min; 3 times), slices were incubated (1 h) in Immunoshot Fine for fluorophore conjugation (0.2% streptavidin-conjugated Alexa Fluor 594). After the final PBS-wash (5 min; 3 times), the sections were mounted on VECTASHIELD (Vector Laboratories, CA, USA), and imaged using a fluorescence microscope (EVOS FL Auto 2 Cell Imaging System; Thermo Fisher Scientific, MA, USA).

Monitoring cardiovascular responses under electrical stimulation of the CeA and/or PVN

In these experiments (and only these), rats were anesthetized with urethane (1.45 g/kg IP). Their rectal

temperature was monitored and maintained at 37 °C using a heating pad (BWT-100; Bio Research Center, Nagoya, Japan). After cannulating the trachea, a polyethylene catheter (PE-50) was inserted into the right femoral artery to record the pulsatile arterial pressure. MAP and HR were calculated from the pulsatile pressure signal using a cardiometer (AP641-G and AT601-G, Nihon Kohden, Tokyo, Japan). The rat's blood flow in the skeletal muscle was measured from the gastrocnemius muscle surface using a laser tissue blood flowmeter (measuring range: radius = 1 mm; Omegaflow FLO-C1, Omegawave Inc., Tokyo, Japan). Skeletal muscle vascular resistance (VR) was calculated according to the following equation: $VR = \text{arterial pressure/muscle blood flow (MBF)}$. These parameters were simultaneously monitored and recorded using the PowerLab system (PowerLab/8s, ADInstruments, Nagoya, Japan).

Electrical stimulation of the CeA and/or PVN

Using the same stereotaxic apparatus and microelectrode described above for CeA lesion experiments, rats ($n = 6$) under urethane anesthesia were electrically stimulated in the right or left CeA (1.8 mm caudal, 3.0 mm lateral to the bregma, and 7.0 mm ventral to the dura) and/or the ipsilateral PVN (1.8 mm caudal, 0.4 mm lateral to the bregma, and 7.7 mm ventral to the dura). Biphasic negative–positive current pulses (200 μA peak, 0.5 ms pulse, 50 Hz, and 30 s duration) were delivered according to the method of Kim et al. (2020). The stimulations were conducted in the following order: CeA, PVN, and both. After acquiring the data, the electrical microstimulation sites were marked by electrolytic lesions (1 mA DC, 5 s). The rats were then perfused with an overdose of urethane.

The brains were removed, sectioned, and imaged for lesion detection exactly as described for CeA lesion experiments above.

Statistical analysis

All values are expressed as mean \pm standard error of the mean. A two-way analysis of variance (ANOVA) with Tukey's honestly significant difference post-hoc test was used to evaluate five measures: the total running time, maximum body temperature (BT), MAP, HR, and time of abrupt increase in MAP (Time-BPinc). We analyzed the significance of the mean differences, ΔBT , ΔMAP , ΔHR , $\Delta\text{Time-BPinc}$, and % of c-Fos expression in CTB-labeled cells, using an unpaired t -test. For the Δtotal running time, a Mann–Whitney U -test was used if normality was not confirmed (Kolmogorov–Smirnov test). To compare cardiovascular responses before and during stimulation of the CeA, PVN, or both, a Student's paired t -test and one-way ANOVA with Tukey's HSD post-hoc test were used. Statistical significance was set at $p < 0.05$. Box plots (produced using the MATLAB function "boxplot") displayed the median value as the center line, mean value as the plot in the box, interquartile range (25th–75th percentiles) as the box range, maximum and minimum data points not

considered as outliers as the whiskers, and individual data for each group as plots outside the box. Outliers were defined as values that were >1.5 times the interquartile range from the bottom or top of the box.

RESULTS

CeA lesions delayed the time at which the abrupt increase of MAP appears in response to high-intensity exercise

We tested whether bilateral CeA lesions prolonged the total running time. Animals ($n = 15$) were divided into sham ($n = 7$) and lesion ($n = 8$) groups. To investigate the effect of CeA lesions on cardiovascular parameters, we recorded arterial pressure and HR during the incremental exercise test. The CeA lesion sites are shown in Fig. 1A. As expected, during the rest period in the pretest, there were no differences between the two groups in both MAP and HR. In the sham control group, MAP at rest in the post-test was significantly higher than that in the pretest (MAP: Sham, Pre: 103.4 ± 1.9 mmHg, Post: 110.5 ± 3.3 mmHg; Lesion, Pre: 104.9 ± 2.5 mmHg, Post: 103.2 ± 1.9 mmHg; $F_{(1,13)} = 27.28$, Pre vs. Post: $p = 0.3460$, Sham vs. Lesion: $p = 0.2321$, interaction: $p < 0.05$, two-way ANOVA; Sham-Pre vs. Sham-Post: $p < 0.05$, post-hoc test). In contrast, in the lesion group, HR at rest in post-test was significantly lower than that in the pre-test (HR: Sham, Pre: 393 ± 9 bpm, Post: 387 ± 9 bpm; Lesion, Pre: 390 ± 10 bpm, Post: 370 ± 6 bpm; $F_{(1,13)} = 367.8$, Pre vs. Post: $p = 0.310$, Sham vs. Lesion: $p = 0.0713$, interaction: $p = 0.305$, two-way ANOVA; Lesion-Pre vs. Lesion-Post: $p < 0.05$, post-hoc test).

As shown in Fig. 1B, the total running time in the CeA lesion group was significantly prolonged in the post-test (67.7 ± 1.9 min) compared to that in the pre-test (57.4 ± 3.5 min) ($p < 0.05$, Tukey's HSD post-hoc test). In contrast, there was no change in the sham control (Pre: 61.0 ± 4.2 min, Post: 60.1 ± 7.3 min), and there was no significant group effect ($F_{(1,13)} = 71.27$, Pre vs. Post: $p = 0.1237$, Sham vs. Lesion: $p = 0.723$, interaction: $p = 0.0939$, two-way ANOVA). Statistical analysis of the pre-post changes in the total running time (another way of looking at the data) shown in Fig. 1C led to the same conclusions (Sham: -0.9 ± 5.1 min, Lesion: 10.3 ± 3.6 min; $F = 0.7394$, Kolmogorov–Smirnov test: $p < 0.05$, Mann–Whitney U -test: $p < 0.05$).

Fig. 2A shows the changes in BT, cardiovascular parameters, and running position in rats, as a function of the exercise time. BT increased for approximately 15 min from the start of exercise, then maintained a plateau for approximately 20 min, then again followed a climb until exhaustion. The time-course of MAP similarly followed a three-phase pattern: increased for the initial approximately 10 min, then held at approximately 120 mmHg until ~ 20 min before the end of exercise, when the MAP exhibited an abrupt increase that held until exhaustion. HR increased with exercise intensity.

With regard to the maximum BT (Fig. 2B), there were no differences between pre- and post-operation in both groups (Sham, Pre: 40.8 ± 0.3 °C, Post: 40.4 ± 0.3 °C;

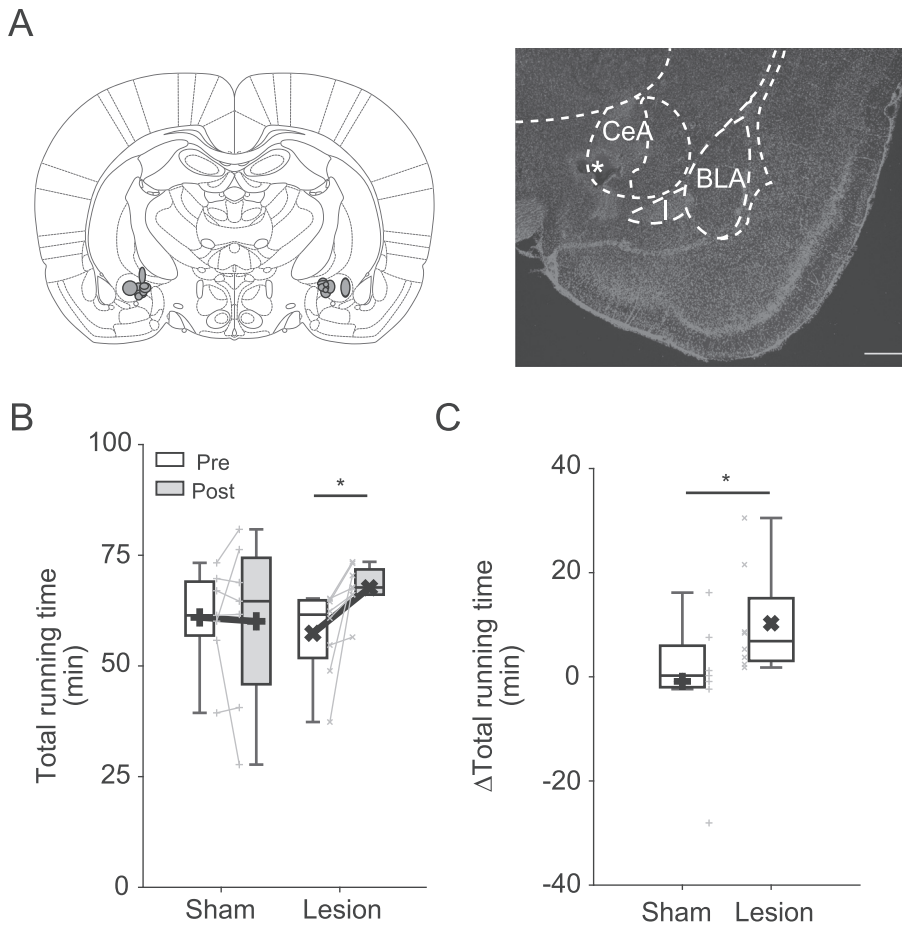


Fig. 1. The effect of CeA lesions on the total treadmill running time. **(A)** Left: Schematic of the CeA lesion sites. Right: Example of a brain slice containing a CeA lesion site (asterisk) imaged on the microscope. Scale bar = 500 μ m. Labeled nuclei of the amygdala: BLA, basolateral nucleus; CeA, central nucleus; I, intercalated nucleus. **(B)** Total running time before and after sham or CeA lesion operations. The plus marks in the white and gray boxes represent the mean values of the sham group and the cross marks represent the mean values of the lesion group. The symbols along the boxes represent individual data: + for the sham rats ($n = 7$) and \times for the lesioned rats ($n = 8$). Significant differences were identified using two-way ANOVA with Tukey's HSD post-hoc test was used. **(C)** Changes of total running time before and after operations (Δ Total running time). Unpaired t -test, $*p < 0.05$. Symbols are the same as those in **(B)**.

Lesion, Pre: 40.3 ± 0.3 $^{\circ}$ C, Post: 40.9 ± 0.3 $^{\circ}$ C; $F_{(1,13)} = 0.5786$, Pre vs. Post: $p = 0.966$, Sham vs. Lesion: $p = 0.786$, interaction: $p = 0.101$, two-way ANOVA). Regarding the maximum BT change before and after the operations, Δ BT (Fig. 2C), there was also no difference between the two groups of rats (Sham: -0.4 ± 0.3 $^{\circ}$ C; Lesion: 0.5 ± 0.4 $^{\circ}$ C, unpaired t -test: $p = 0.0938$).

Analysis of the maximum MAP had similar results. Maximum MAP was not changed by the operations in either group (Fig. 2D; Sham, Pre: 145.7 ± 5.5 mmHg, Post: 142.6 ± 5.8 mmHg; Lesion, Pre: 140.4 ± 6.7 mmHg, Post: 138.6 ± 2.9 mmHg; $F_{(1,13)} = 197.39$, Pre vs. Post: $p = 0.429$, Sham vs. Lesion: $p = 0.647$, interaction: $p = 0.904$, two-way ANOVA). Nor was the MAP change before and after the operations (Δ MAP, Fig. 2E) different between the two groups (Sham: -3.1 ± 6.9 mmHg, Lesion: -1.8 ± 7.5 mmHg; unpaired t -test: $p = 0.9028$).

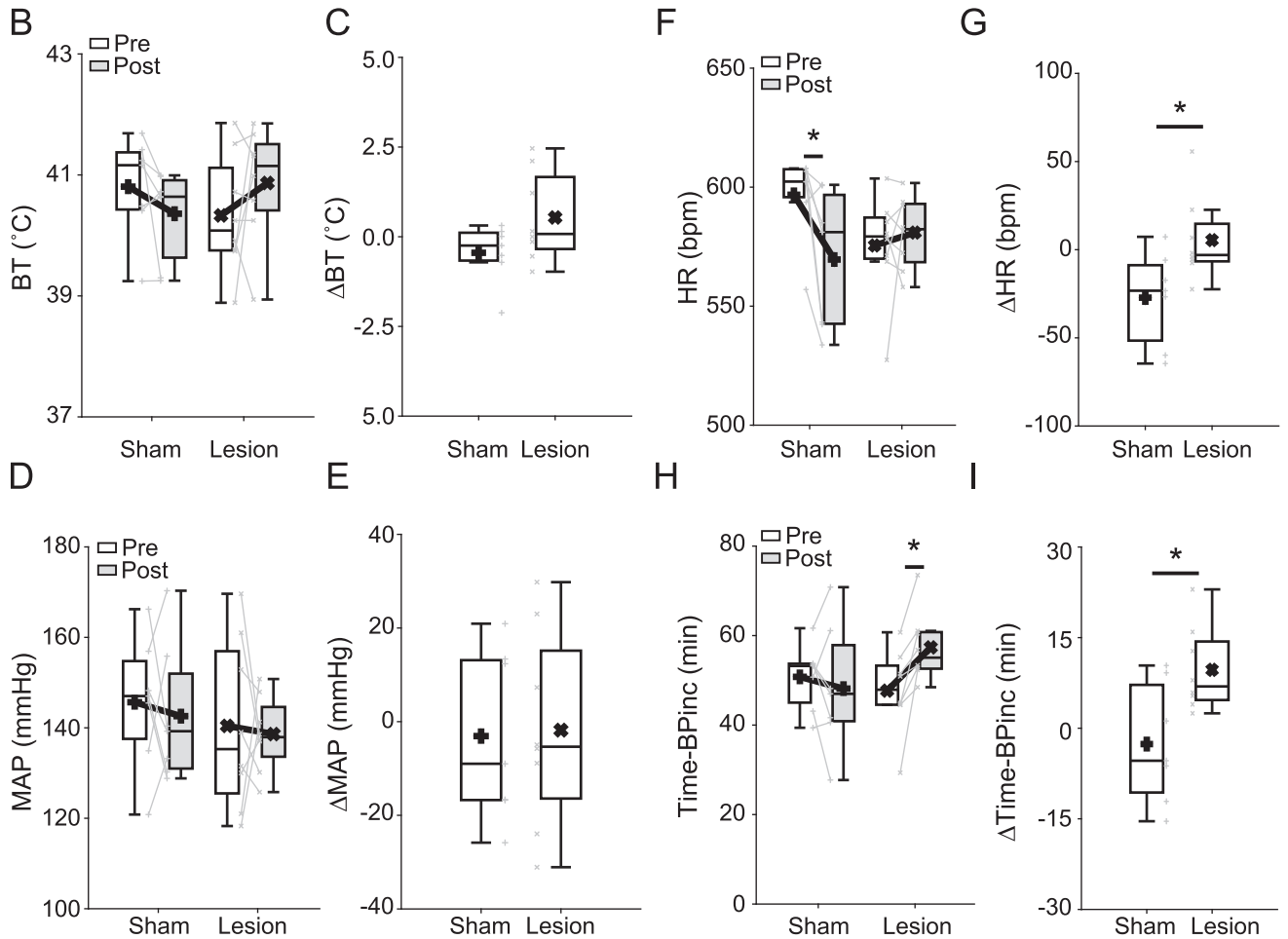
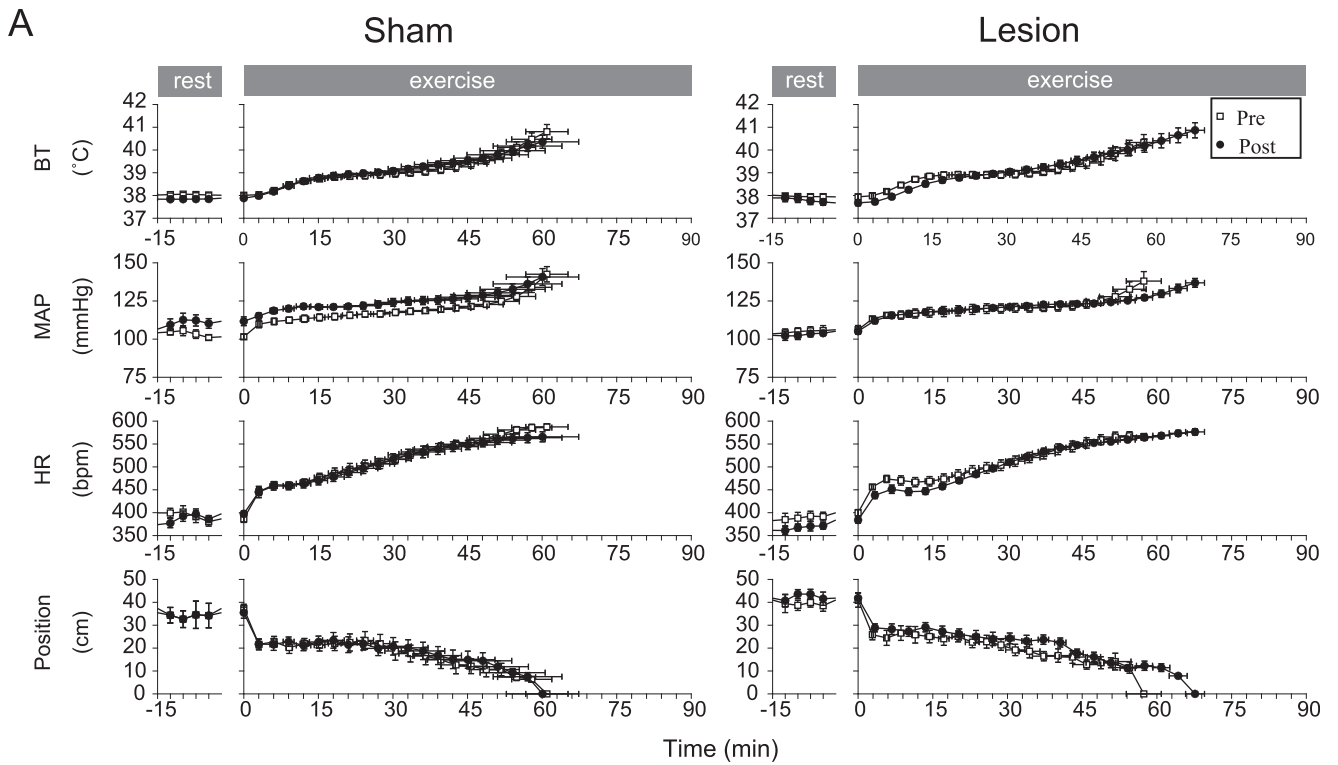
In contrast, an interaction but no main effects were found for the maximum HR (Fig. 2F; Sham, Pre: 597 ± 7 bpm, Post: 570 ± 11 bpm; Lesion, Pre: 576 ± 8 bpm, Post: 581 ± 5 bpm; $F_{(1,13)} = 317.50$, Pre vs. Post: $p = 0.5910$, Sham vs. Lesion: $p = 0.1558$, interaction: $p < 0.05$, two-way ANOVA). Accordingly, the post-hoc test revealed that the maximum HR in the Sham group was significantly higher before the operation than after ($p < 0.05$). As expected, the differences in the maximum HR before and after the operations (i.e., Δ HR) were significantly different between the two groups (Fig. 2G; Sham: -27 ± 10 bpm, Lesion: 5 ± 9 bpm; unpaired t -test: $p < 0.05$).

Regarding the time at which the MAP exhibited an abrupt increase during high-intensity exercise, BPinc (Fig. 2H), there was an interaction but no main effects (Sham, Pre: 50.8 ± 2.8 min, Post: 48.1 ± 5.3 min; Lesion, Pre: 47.7 ± 3.3 min, Post: 57.4 ± 2.8 min; $F_{(1,13)} = 36.28$, Pre vs. Post: $p = 0.5210$, Sham vs. Lesion: $p = 0.0973$, interaction: $p < 0.05$, two-way ANOVA). According to the post-hoc test, BPinc significantly increased after a CeA lesion ($p < 0.05$). The before-after time difference, Δ Time-BPinc (Fig. 2I), was also significantly different between the two groups of rats (Sham: -2.6 ± 3.8 min, Lesion: 9.7 ± 2.5 min; unpaired t -test: $p < 0.05$), suggesting that

CeA lesions delayed the time at which the abrupt increase in arterial pressure appears in response to high-intensity exercise.

NTS-projecting CeA and PVN neurons were activated by high-intensity exercise

We examined whether high-intensity exercise activates the NTS-projecting neurons in the CeA and PVN. We labeled those neurons in rats ($n = 11$) with retrograde axon tracer cholera toxin subunit B (CTB) injected into the NTS (200 nl; Fig. 3A). Five days later, the animals were subjected to an incremental exercise test. The average total running time to exhaustion was 74.9 ± 2.2 minutes. The brains of the animals were processed postmortem to detect neurons in the two nuclei that were dually immunolabeled with fluorophore-conjugated antibodies, one against the retrograde tracer



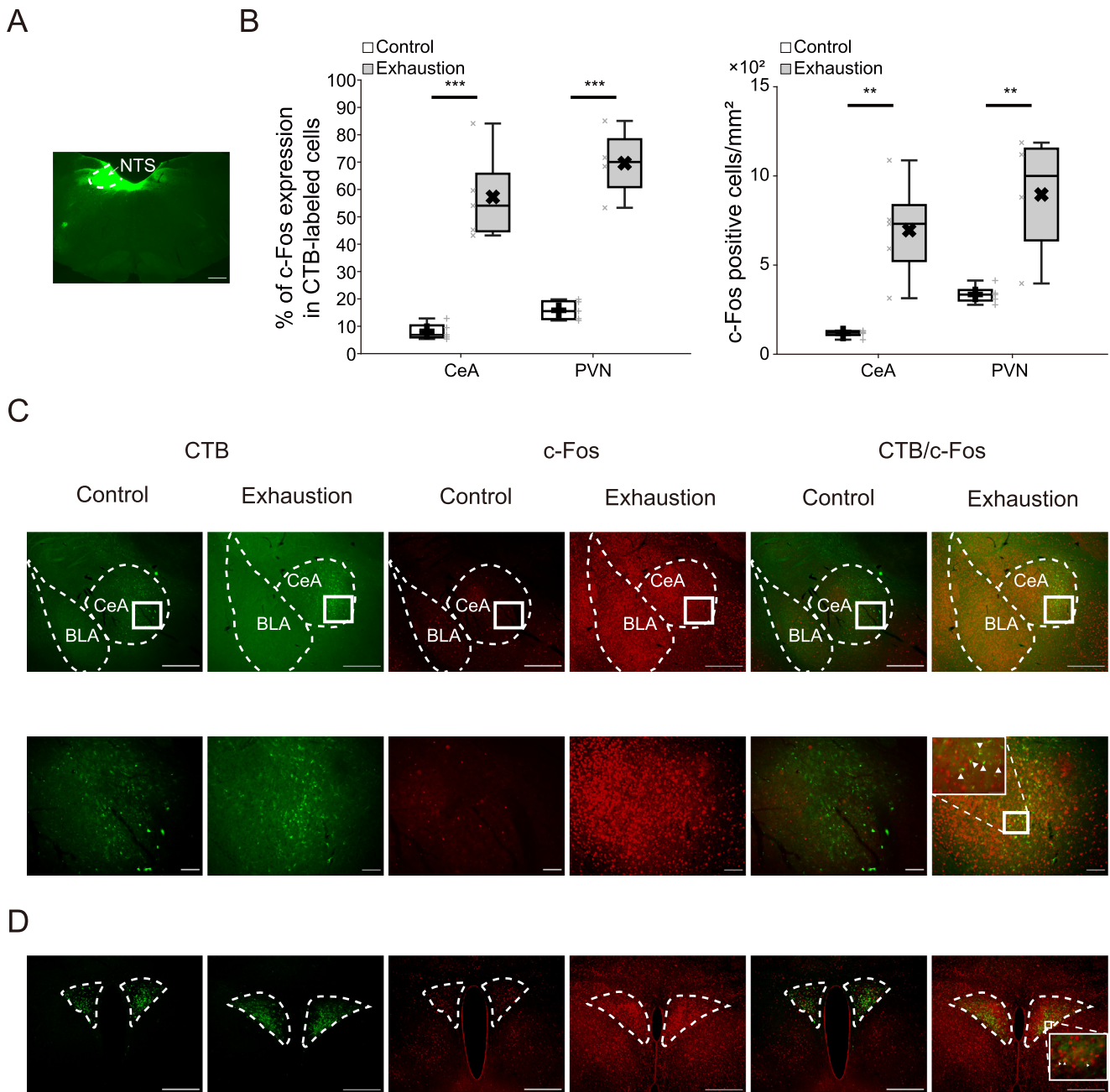
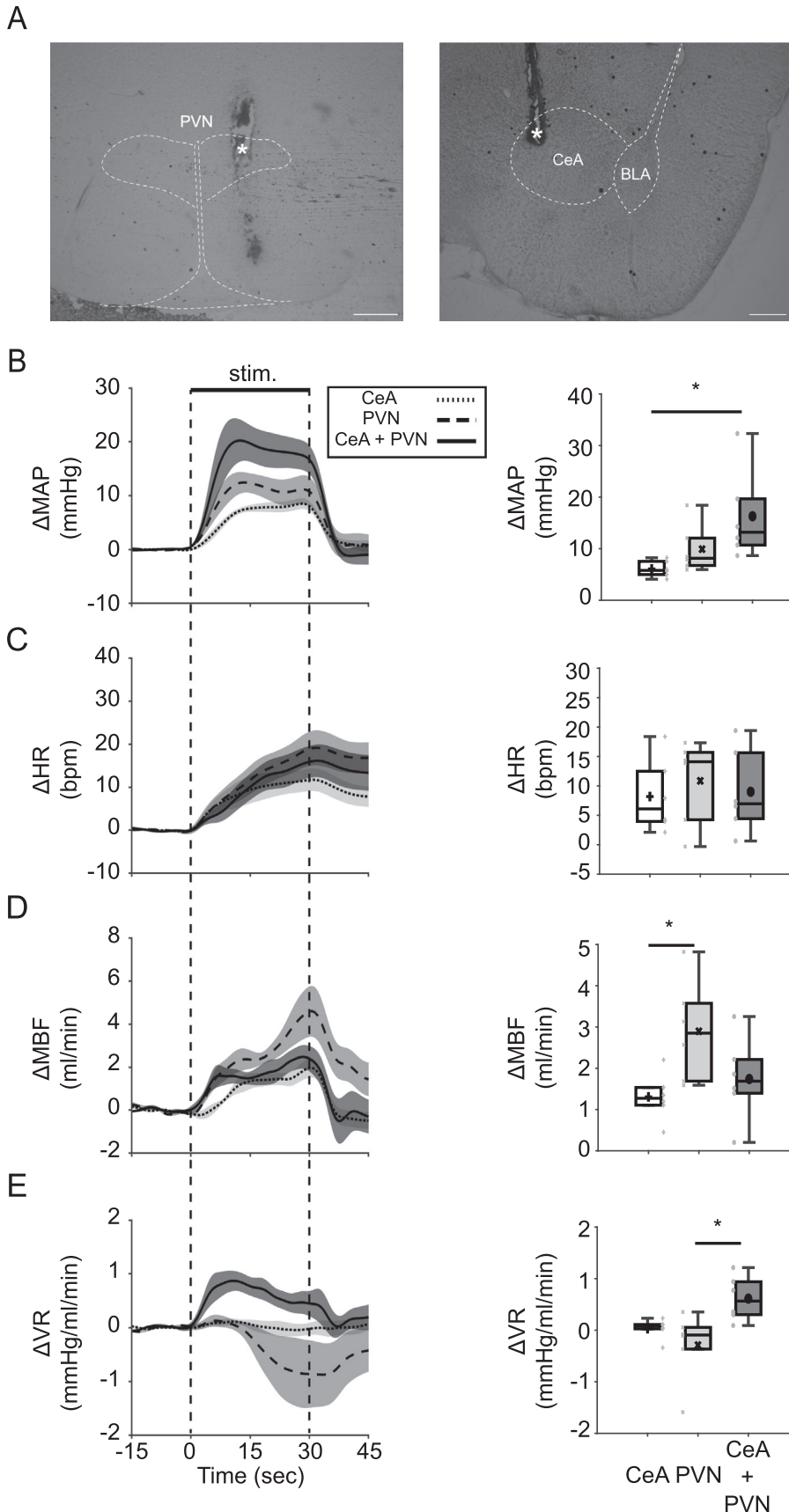


Fig. 3. Co-expression of two fluorescent labels, c-Fos for activity and Cholera toxin subunit B (CTB) for NTS afferents, in the CeA and PVN after the maximum incremental exercise test. **(A)** Representative NTS injection site of CTB imaged on the fluorescent microscope. Scale bar = 500 μm . **(B)** (Left) The percentage of c-Fos expressing cells within the CTB-labeled populations in CeA (Exhaustion, $n = 5$; Control, $n = 5$), and in PVN (Exhaustion, $n = 4$; Control, $n = 5$). (Right) c-Fos-expressing cells (per mm^2) in the CeA (Exhaustion, $n = 5$; Control, $n = 5$) and PVN (Exhaustion, $n = 4$; Control, $n = 5$). Unpaired t -test, $^{***}p < 0.001$ and $^{**}p < 0.01$. **(C)** Representative images showing neurons double labeled for CTB (green) and c-Fos (red) in the CeA. The images at the bottom zoom in on areas delineated by squares in the upper photographs. Neurons double-stained with anti-CTB and anti-c-Fos antibodies are indicated by triangles. Scale bars = 500 μm , top images; 100 μm , zoomed images. **(D)** Double labeling in the PVN, marked as in **(B, C)**. Scale bar = 500 μm . (For interpretation of the references to colour in this figure legend, the reader is referred to the web version of this article.)

Fig. 2. The effect of CeA lesions on the cardiovascular responses to the incremental exercise test. **(A)** Time-dependent change(s) in BT, MAP, HR, and position in running of rats during the incremental exercise test before and after the surgical operations (Sham: $n = 7$; Lesions: $n = 8$). Data were sampled at 20 equal time intervals set to 5% of the maximum exercise time (100%). Plots on the left summarize data for the **(B)** maximum BT, **(D)** maximum MAP, **(F)** maximum HR, and **(H)** Time-BPinc. Data are shown as group averages (symbols in the boxes) and measurements in individual rats (+ for the sham; \times for the lesion rats; along the boxes). A two-way ANOVA with Tukey's HSD post-hoc test was used for the statistical significance of mean differences. On the right, similarly organized, are the pre-post-operation maximum differences **(C)** ΔBT , **(E)** ΔMAP , **(G)** ΔHR , and **(I)** $\Delta\text{Time-BPinc}$. For these data, the unpaired t -test was used ($^*p < 0.05$). Symbols are the same as those in **(B)**.



CTB, and another against a marker for neuronal activation, c-Fos.

As shown in Fig. 3B (right), high-intensity exercise dramatically increased the number of neurons expressing c-Fos in both the CeA (CeA-Control: 116 ± 8 cells/mm², CeA-Exhaustion: 696 ± 112 cells/mm², $p < 0.01$) and PVN (PVN-Control: 335 ± 20 cells/mm², PVN-Exhaustion: 896 ± 155 cells/mm², $p < 0.01$). Notably, during high-intensity exercise, the expression of c-Fos in the CeA was most prominent in the lateral region (Fig. 3C; top, third photograph from the right), whereas in the PVN, it was most prominent in the parvocellular division (Fig. 3D; third photograph from the right). In contrast, during high-intensity exercise, among the CTB-labeled neurons in the CeA, the neurons expressing c-Fos were mainly located in the medial division of the CeA (Fig. 3C; top, photograph on the right), whereas among the CTB-labeled neurons in the PVN, the neurons expressing c-Fos were mainly located in the lateral part of the PVN (Fig. 3D; photograph on the right). Importantly, high-intensity exercise also dramatically increased the fraction of c-Fos-positive neurons among the CTB-labeled neurons both in the CeA (CeA-Control: $8.13 \pm 1.37\%$, CeA-Exhaustion: $57.25 \pm 7.35\%$, $p < 0.001$) and PVN (PVN-Control: $15.83 \pm 1.56\%$, PVN-Exhaustion: $69.61 \pm 6.52\%$, $p < 0.001$, Fig. 3B left). Thus, while only a small minority of NTS-projecting neurons in the CeA and PVN was activated when the animals were in sedentary condition, under high-intensity exercise the majority were activated in both the CeA and PVN.

Simultaneous electrical microstimulation of the CeA and PVN of anesthetized rats increased not only MAP, HR, and MBF, but also VR

We investigated the effect of electrical microstimulation of the CeA, PVN, or simultaneous stimulation of both brain areas (CeA + PVN) on the

cardiovascular response by measuring MAP, HR, MBF, and VR in anesthetized rats ($n = 6$). Averaged data for 15 s before electrical microstimulation and for 30 s during stimulation to the target brain area(s) were assessed.

As seen in Fig. 4A-Left, and verified by Student's paired t -test, MAP was significantly increased by the electrical microstimulation to the CeA (Pre: 71.1 ± 3.7 mmHg, Post: 77.1 ± 4.0 mmHg; $p < 0.001$), to the PVN (Pre: 72.2 ± 4.7 mmHg, Post: 82.1 ± 4.2 mmHg; $p < 0.01$), and to both areas (CeA + PVN, Pre: 73.9 ± 4.8 mmHg, Post: 90.1 ± 3.3 mmHg; $p < 0.01$). The pressor response was greatest for the CeA + PVN stimulation, with the MAP increase, Δ MAP (Fig. 4A-Right), being approximately equal to a linear summation of the increases found for the stimulation of the individual nuclei (CeA: 6.1 ± 0.6 mmHg, PVN: 9.9 ± 1.7 mmHg, CeA + PVN: 16.3 ± 3.2 mmHg; $F_{(2, 14)} = 35.73$, $p < 0.05$, one-way ANOVA; CeA vs. CeA + PVN, $p < 0.05$, Tukey's HSD).

HR (Fig. 4B-Left) also significantly, but only slightly, increased in response to electrical microstimulation in all cases (CeA, Pre: 449 ± 16 bpm, Post: 457 ± 16 bpm, $p < 0.01$; PVN, Pre: 469 ± 16 bpm, Post: 480 ± 14 bpm, $p < 0.05$; CeA + PVN, Pre: 472 ± 13 bpm, Post: 481 ± 12 bpm, $p < 0.05$). However, the stimulation-induced HR change, Δ HR (Fig. 4B-Right), was not different among the three groups (CeA: 8 ± 2 bpm, PVN: 11 ± 3 bpm, simultaneous CeA + PVN: 9 ± 3 bpm; $F_{(2, 14)} = 49.36$, $p = 0.799$, one-way ANOVA).

MBF, shown in Fig. 4C-Left, was also significantly, but only slightly, increased by electrical microstimulation in all cases (CeA, Pre: 18.6 ± 1.9 ml/min, Post: 19.9 ± 2.0 ml/min, $p < 0.01$; PVN, Pre: 16.0 ± 1.8 ml/min, Post: 18.8 ± 1.6 ml/min, $p < 0.01$; CeA + PVN, Pre: 15.8 ± 1.6 ml/min, Post: 17.5 ± 1.9 ml/min, $p < 0.01$). Interestingly, the stimulation-induced MBF change, Δ MBF (Fig. 4C-Right), due to stimulation in the PVN was approximately two times greater than Δ MBF due to CeA stimulation alone or in combination with PVN (CeA: 1.3 ± 0.2 ml/min, PVN: 2.9 ± 0.5 ml/min, CeA + PVN: 1.7 ± 0.4 ml/min; $F_{(2, 14)} = 1.014$, $p < 0.05$, one-way ANOVA; CeA vs. PVN, $p < 0.05$, Tukey's HSD).

VR, shown in Fig. 4D-Left, was not affected by electrical microstimulation of the CeA (Pre: 4.21 ± 0.74 mmHg/ml/min, Post: 4.24 ± 0.67 mmHg/ml/min, $p = 0.660$) or the PVN (Pre: 5.07 ± 0.87 mmHg/ml/min, Post: 4.78 ± 0.67 mmHg/ml/min; $p = 0.353$). In contrast, simultaneous CeA + PVN stimulation resulted in a significant increase in VR (Pre: 5.14 ± 0.78 mmHg/ml/min, Post: 5.75 ± 0.82 mmHg/ml/min; $p < 0.05$). The change in VR, Δ VR, shown in Fig. 4D-Right, was

significantly greater with CeA + PVN stimulation than with stimulation of the PVN alone (CeA: 0.03 ± 0.07 mmHg/ml/min, PVN: -0.29 ± 0.25 mmHg/ml/min; CeA + PVN: 0.61 ± 0.16 mmHg/ml/min; $F_{(2, 14)} = 0.242$, $p < 0.05$, one-way ANOVA, PVN vs. CeA + PVN, $p < 0.05$, Tukey's HSD).

DISCUSSION

We examined the hypothesis that the activation of the CeA during high-intensity exercise affects cardiovascular regulation via the PVN and NTS interactions, as a result affecting maximum exercise performance. First, we measured the total running time and cardiovascular responses before and after CeA lesions. We found that CeA lesions significantly increased the total running time to exhaustion. Moreover, the CeA lesions delayed the time at which the abrupt increase in MAP appeared in response to high-intensity exercise. Second, we showed that more than half of the NTS-projecting neurons in both the CeA and PVN were activated by high-intensity exercise. Finally, we measured the cardiovascular responses to electrical microstimulation of the CeA and/or PVN in anesthetized rats. We found that CeA or PVN stimulation alone significantly increased MAP, HR, and notably also MBF, but left the VR unaffected. However, simultaneous stimulation of CeA and PVN significantly increased VR in addition to MAP, HR, and MBF. From these three experiments, our data support the idea that the activation of the CeA in response to high-intensity exercise affects both cardiovascular regulation and total running time. The abrupt increase in MAP observed during high-intensity exercise may be attributed to vasoconstriction or increased vascular tone in the skeletal muscle due to increased sympathetic excitation caused by the simultaneous activation of the CeA and PVN. Moreover, the cardiovascular responses observed during high-intensity exercise may represent brain-muscle reciprocal interactions during fatigue; this will need to be elucidated in the future.

This study showed that CeA lesions increased the total running time and delayed the time at which an abrupt increase in MAP appeared in response to high-intensity exercise. Together with our histological and acute physiological studies, these results suggest that activation of the CeA may affect maximum exercise performance through hyperstimulation of sympathetic nerve activity mediated by the PVN and NTS. The PVN is known as the "master controller" of the sympathetic nervous system (Feetham et al., 2018), and it directly and indirectly regulates sympathetic preganglionic neurons in the intermediolateral cell column (Appel and Elde, 1988; Shaffon et al., 1998; Pyner and Coote,

Fig. 4. Changes in cardiovascular parameters following electrical microstimulation of the CeA, PVN, or both brain areas. **(A)** Example of a brain slice showing the CeA (right) and PVN (left) lesion sites (*) imaged using a microscope. Scale bar = 500 μ m. **(B–E)** On the left, curves plot the time-dependent changes from the baseline levels, averaged across animals, in response to electrical microstimulation of the CeA only (dotted line), PVN only (dashed line), and CeA + PVN simultaneously (solid line). On the right, figures show average data ($n = 6$) of changes in the cardiovascular parameters induced by electrical microstimulation. **(B)** Δ MAP, **(C)** Δ HR, **(D)** Δ MBF, and **(E)** Δ VR. One-way ANOVA. * $p < 0.05$. The symbols in the boxes show the mean values of each group, and the symbols along the boxes show the individual data of each group.

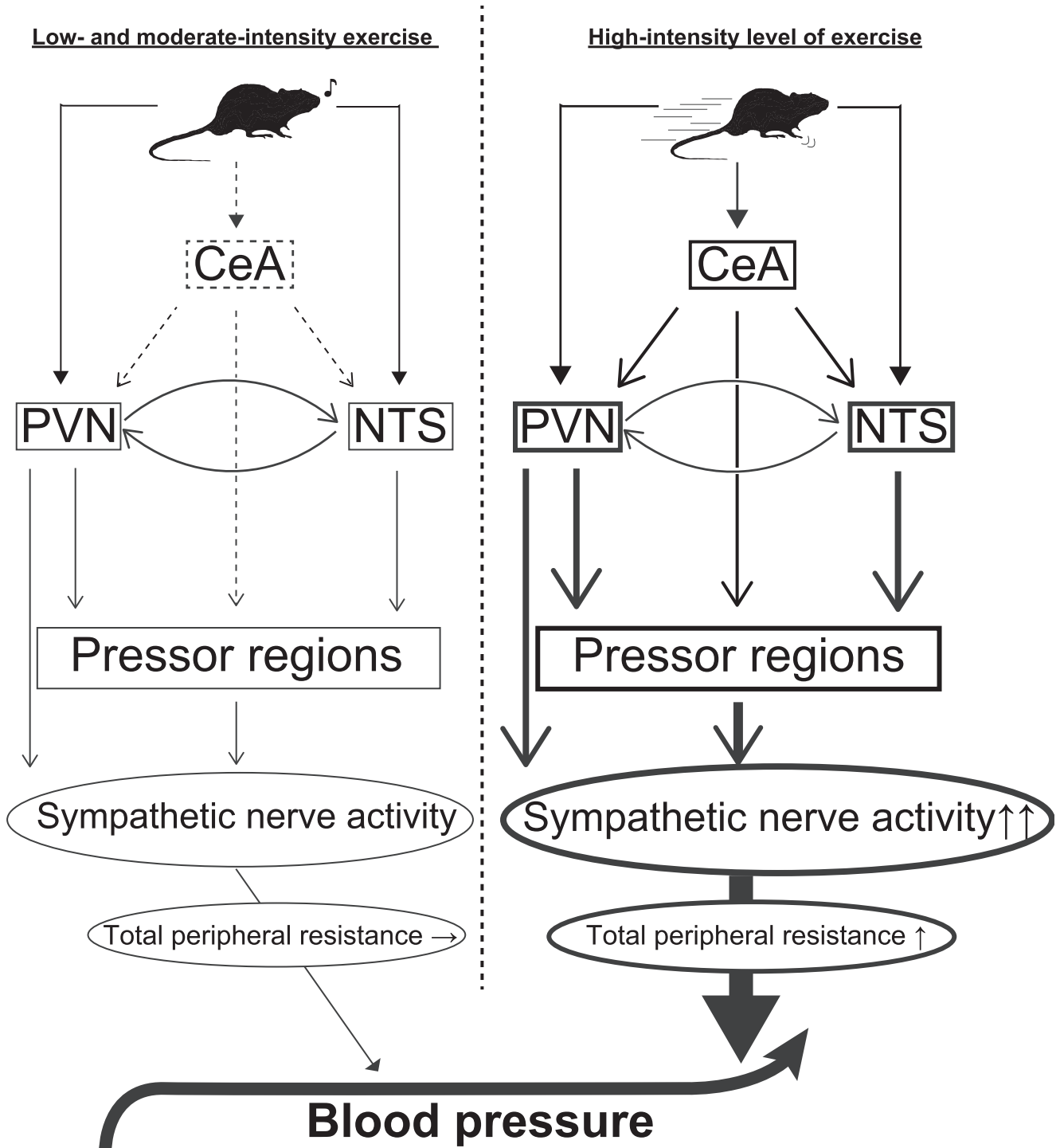


Fig. 5. Hypothetical schema of the central mechanisms of cardiovascular regulation during low- and moderate-intensity exercise (left) and high-intensity exercise (right). During low- and moderate-intensity exercise (left), the reciprocal connections between the NTS and PVN perform cardiovascular regulation, and both brain areas control the autonomic outflows, thereby modulating and maintaining arterial pressure at a constant level. However, during high-intensity exercise (right), the activated CeA affects the neuronal activity of the PVN and NTS circuits. The resulting override of sympathetic nerve activity disrupts hemodynamic homeostasis during high-intensity exercise.

2000). In the indirect path, the PVN regulates sympathetic pre-motor neurons in the rostral ventrolateral medulla (RVLM) (Pyner and Coote, 2000; Bowman et al., 2013), and regulates NTS neurons (Dampney et al., 2018). The NTS is known as a cardiovascular control center that modulates the baroreceptor reflex via regulating both

sympathetic and parasympathetic nerve activity (Waki, 2012). A single bout of exercise is known to induce pressor and tachycardiac responses by modulating the baroreceptor reflex (Miki et al., 2003). Barosensitive neurons of the NTS regulate GABAergic neurons in the caudal ventrolateral medulla (CVLM), which in turn innervate

sympathetic pre-motor neurons in the RVLM (Waki, 2012). Previous studies have shown that the reciprocal connections between the NTS and PVN constitute the anatomical basis for cardiovascular regulation during exercise, and this circuit may be an important component of the central command of cardiovascular regulation in general (Michelini and Stern, 2009). Specifically, the NTS-PVN circuit is thought to control autonomic outflows, ultimately modulating and maintaining arterial pressure at a constant level during exercise of low-to-moderate-intensity (Fig. 5).

However, during high-intensity exercise, activation of the CeA may affect the cardiovascular homeostasis seen during low-to-moderate-intensity exercise. It was previously shown that the CeA is activated only during high-intensity exercise, but not moderate-intensity exercise (Kim et al., 2020). It is known that CeA neurons send afferents to neurons in the PVN and RVLM (Silverman et al., 1981; Saha et al., 2005) and in the NTS, as found in this study. Activation of the CeA during high-intensity exercise may affect the neuronal activity of the PVN, as well as the NTS (Gray et al., 1989; Fadok et al., 2018), and the interruption of the PVN and NTS circuits may cause an overdrive of sympathetic nerve activity. As a result, high-intensity exercise may increase arterial pressure due to an increase in VR (Fig. 5). Moreover, disruption of the hemodynamic homeostasis in the active muscles may lead to accumulation of metabolites, muscle fatigue and negative emotions (i.e., brain-muscle interactions in fatigue), contributing to exhaustion.

It should be noted that although the CeA lesions delayed the onset time of abrupt arterial pressure increase, the pressor response itself remained even after the CeA lesions. This suggests that brain regions other than the CeA may also be involved in the cardiovascular responses during high-intensity exercise, and further research is required to identify these brain areas and detailed neuronal mechanisms.

One of the limitations of this study was the use of mild electrical microstimulation (foot shocks) to encourage rats to run on the treadmill. Many previous studies have used foot shocks for fear-conditioning acquisition and have investigated the functional roles of the CeA in the process (Haubensak et al., 2010; Li et al., 2013; Han et al., 2015; Tovote et al., 2015; Fadok et al., 2018). Therefore, c-Fos expression in the CeA induced by the high-intensity running test in this study might partially reflect the effect of the mild electric foot shock itself, confounding the effect of physical/mental exhaustion that result from the maximum running test. In fact, a high level of c-Fos expression after exhaustion was mainly found in the lateral part of the CeA and the parvocellular division of the PVN, which are known to have corticotropin-releasing hormone-containing neurons (Aguilera and Liu, 2012; Walker, 2021). This suggests that the exercise test performed in this study was a major stress on running rats and the underlying fear of electric shocks may be partly responsible for the stress responses. Our study cannot prove that the NTS-projecting CeA and/or PVN neurons are involved in cardiovascular responses during high-intensity exercise but it does provide a correlation

between these two phenomena. We used electrical microstimulation to determine the potential autonomic mechanisms of cardiovascular responses and estimate how they affect maximum exercise performance through the CeA. An advantage of electrical microstimulation is its high temporal resolution compared with that of chemical stimulation, whereas a weakness of this method is the possibility of causing lesions or stimulation of axons of passage as well as cell bodies at the stimulation sites. Further studies using techniques capable of direct manipulating of neuronal activity in behaving animals, such as optogenetics and chemogenetic approaches to assess the functional relevance of the specific CeA to NTS projection (e.g., a dual viral approach combining retrograde Cre-expressing adeno-associated virus (AAV) in combination with Cre-dependent Gs/Gq AAVs), will be required. Finally, this study was not designed to be able to determine whether hemodynamic changes during high-intensity exercise are a cause or consequence of central fatigue. Further studies will be required to distinguish the two possibilities and test our hypothesis that hemodynamic changes are involved in the brain-muscle reciprocal interactions during fatigue. Specifically, it will be necessary to (1) investigate whether VR in the active muscle increases during high-intensity exercise, which facilitates metabolite production in the muscle; and (2) determine whether afferent information from the muscle metaboreceptors stimulates the amygdala or other emotion centers.

In conclusion, the activation of the CeA during high-intensity exercise affects cardiovascular parameters and maximum exercise performance. Moreover, autonomic control of the CeA in modulating the PVN-NTS pathway may be involved in the cardiovascular responses via VR regulation in the active muscle.

AUTHORS' CONTRIBUTIONS

K.T., K.Y., and H.W. conceived and designed the research; K.T. and K.Y. performed the experiments; K. T. analyzed the data; K.T., K.Y., and H.W. interpreted the experimental results; K.T. prepared the figures; K.T. drafted the manuscript; K.T. and H.W. edited and revised the manuscript. All authors have read and approved the final version of manuscript.

GRANTS

This study was supported by a Grant-in-Aid for a Japan Society for the Promotion of Science Research Fellow (19J22706; to K.T.), a Grant-in-Aid for Scientific Research (C) (19K11449; to H.W.), the MEXT-supported Program for the Strategic Research Foundation at Private Universities 2014–2018 (S1411008; Juntendo University), and the MEXT Private University Research Branding Project (Juntendo University).

DISCLOSURES

The authors declare that there is no conflict of interest.

REFERENCES

- Aguilera G, Liu Y (2012) The molecular physiology of CRH neurons. *Front Neuroendocrinol* 33(1):67–84.
- Allen DG, Lamb GD, Westerblad H (2008) Skeletal muscle fatigue: cellular mechanisms. *Physiol Rev* 88(1):287–332.
- Appel NM, Elde RP (1988) The intermediolateral cell column of the thoracic spinal cord is comprised of target-specific subnuclei: evidence from retrograde transport studies and immunohistochemistry. *J Neurosci* 8(5):1767–1775.
- Baxter MG, Murray EA (2002) The amygdala and reward. *Nat Rev Neurosci* 3(7):563–573.
- Bowman BR, Kumar NN, Hassan SF, McMullan S, Goodchild AK (2013) Brain sources of inhibitory input to the rat rostral ventrolateral medulla. *J Comp Neurol* 521(1):213–232.
- Ciocchi S, Herry C, Grenier F, Wolff SBE, Letzkus JJ, Vlachos I, Ehrlich I, Sprengel R, Deisseroth K, Stadler MB, Müller C, Lüthi A (2010) Encoding of conditioned fear in central amygdala inhibitory circuits. *Nature* 468(7321):277–282.
- Dampney RA, Michelini LC, Li D-P, Pan H-L (2018) Regulation of sympathetic vasomotor activity by the hypothalamic paraventricular nucleus in normotensive and hypertensive states. *Am J Physiol Heart Circ Physiol* 315(5):H1200–H1214.
- DiFeliceantonio AG, Berridge KC (2012) Which cue to 'want'? Opioid stimulation of central amygdala makes goal-trackers show stronger goal-tracking, just as sign-trackers show stronger sign-tracking. *Behav Brain Res* 230(2):399–408.
- Duvarci S, Pare D (2014) Amygdala microcircuits controlling learned fear. *Neuron* 82(5):966–980.
- Duvarci S, Popa D, Pare D (2011) Central amygdala activity during fear conditioning. *J Neurosci* 31(1):289–294.
- Fadok JP, Markovic M, Tovote P, Lüthi A (2018) New perspectives on central amygdala function. *Curr Opin Neurobiol* 49:141–147.
- Feetham CH, O'Brien F, Barrett-Jolley R (2018) Ion channels in the paraventricular hypothalamic nucleus (PVN); emerging diversity and functional roles. *Front Physiol* 9:760.
- Fitts RH (1994) Cellular mechanisms of muscle fatigue. *Physiol Rev* 74(1):49–94.
- Gasparini S, Howland JM, Thatcher AJ, Geerling JC (2020) Central afferents to the nucleus of the solitary tract in rats and mice. *J Comp Neurol* 528(16):2708–2728.
- Gray TS, Carney ME, Magnuson DJ (1989) Direct projections from the central amygdaloid nucleus to the hypothalamic paraventricular nucleus: possible role in stress-induced adrenocorticotropin release. *Neuroendocrinology* 50:433–446.
- Gu Y, Piper WT, Branigan LA, Vazey EM, Aston-Jones G, Lin L, LeDoux JE, Sears RM (2020) A brainstem-central amygdala circuit underlies defensive responses to learned threats. *Mol Psychiatry* 25(3):640–654.
- Han S, Soleiman MT, Soden ME, Zweifel LS, Palmiter RD (2015) Elucidating an affective pain circuit that creates a threat memory. *Cell* 162(2):363–374.
- Haubensak W, Kunwar PS, Cai H, Ciocchi S, Wall NR, Ponnusamy R, Biag J, Dong H-W, Deisseroth K, Callaway EM, Fanselow MS, Lüthi A, Anderson DJ (2010) Genetic dissection of an amygdala microcircuit that gates conditioned fear. *Nature* 468(7321):270–276.
- Kannan H, Yamashita H (1985) Connections of neurons in the region of the nucleus tractus solitarius with the hypothalamic paraventricular nucleus: Their possible involvement in neural control of the cardiovascular system in rats. *Brain Research* 329(1-2):205–212.
- Kim J, Yamanaka K, Tsukioka K, Waki H (2020) Potential role of the amygdala and posterior claustrum in exercise intensity-dependent cardiovascular regulation in rats. *Neuroscience* 432:150–159.
- Krabbe S, Gründemann J, Lüthi A (2018) Amygdala inhibitory circuits regulate associative fear conditioning. *Biol Psychiatry* 83(10):800–809.
- LeDoux J (2007) The amygdala. *Curr Biol* 17(20):R868–R874.
- Li H, Penzo MA, Taniguchi H, Kopec CD, Huang ZJ, Li Bo (2013) Experience-dependent modification of a central amygdala fear circuit. *Nat Neurosci* 16(3):332–339.
- Lima PMA, Campos HO, Fóscolo DRC, Szawka RE, Wanner SP, Coimbra CC (2019) The time-course of thermoregulatory responses during treadmill running is associated with running duration-dependent hypothalamic neuronal activation in rats. *Brain Struct Funct* 224(8):2775–2786.
- Mahler SV, Berridge KC (2012) What and when to "want"? Amygdala-based focusing of incentive salience upon sugar and sex. *Psychopharmacology (Berl)* 221(3):407–426.
- Mathis A, Mamidanna P, Cury KM, Abe T, Murthy VN, Mathis MW, Bethge M (2018) DeepLabCut: markerless pose estimation of user-defined body parts with deep learning. *Nat Neurosci* 21(9):1281–1289.
- Michelini LC, Stern JE (2009) Exercise-induced neuronal plasticity in central autonomic networks: role in cardiovascular control. *Exp Physiol* 94:947–960.
- Miki K, Yoshimoto M, Tanimizu M (2003) Acute shifts of baroreflex control of renal sympathetic nerve activity induced by treadmill exercise in rats. *J Physiol* 548(1):313–322.
- Pyner S, Coote JH (2000) Identification of branching paraventricular neurons of the hypothalamus that project to the rostral ventrolateral medulla and spinal cord. *Neuroscience* 100(3):549–556.
- Rogers RC, Fryman DL (1988) Direct connections between the central nucleus of the amygdala and the nucleus of the solitary tract: an electrophysiological study in the rat. *J Auton Nerv Syst* 22(1):83–87.
- Saha S (2005) Role of the central nucleus of the amygdala in the control of blood pressure: descending pathways to medullary cardiovascular nuclei. *Clin Exp Pharmacol Physiol* 32(5-6):450–456.
- Saha S, Drinkhill MJ, Moore JP, Batten TF (2005) Central nucleus of amygdala projections to rostral ventrolateral medulla neurones activated by decreased blood pressure. *Eur J Neurosci* 21:1921–1930.
- Shafiq AD, Ryan A, Badoer E (1998) Neurons in the hypothalamic paraventricular nucleus send collaterals to the spinal cord and to the rostral ventrolateral medulla in the rat. *Brain Res* 801(1-2):239–243.
- Silverman AJ, Hoffman DL, Zimmerman EA (1981) The descending afferent connections of the paraventricular nucleus of the hypothalamus (PVN). *Brain Res Bull* 6(1):47–61.
- Tovote P, Fadok JP, Lüthi A (2015) Neuronal circuits for fear and anxiety. *Nat Rev Neurosci* 16(6):317–331.
- Tsukioka K, Yamanaka K, Waki H (2019) Effects of bilateral lesions in the central amygdala on spontaneous baroreceptor reflex in conscious rats. *JPFMS* 8(1):45–50.
- Walker LC (2021) A balancing act: the role of pro- and anti-stress peptides within the central amygdala in anxiety and alcohol use disorders. *J Neurochem* 157(5):1615–1643.
- Waki H (2012) Central mechanisms of cardiovascular regulation during exercise: Integrative functions of the nucleus of the solitary tract. *J Phys Fitness Sports Med* 1(2):253–261.
- Waki H, Kasparov S, Katahira K, Shimizu T, Murphy D, Paton JF (2003) Dynamic exercise attenuates spontaneous baroreceptor reflex sensitivity in conscious rats. *Exp Physiol* 88:517–526.
- Westerblad H, Lee JA, Lannergren J, Allen DG (1991) Cellular mechanisms of fatigue in skeletal muscle. *Am J Physiol* 261(2):C195–C209.
- Yamanaka K, Takagishi M, Kim J, Gouraud SS, Waki H (2018) Bidirectional cardiovascular responses evoked by microstimulation of the amygdala in rats. *J Physiol Sci* 88(3):233–242.